Proc. Instn Civ. Engrs, Part 2, 1988, **85**, Mar., 161–184

PAPER 9292 STRUCTURAL ENGINEERING GROUP

Cable design for continuous prestressed concrete bridges

C. J. BURGOYNE, MA, PhD, DIC, MICE*

The Paper discusses the criteria which govern the cable design in continuous prestressed concrete beams. A rigorous analysis is used to show that Low's condition regarding the shortening of the extreme fibres is a particular case of a more general condition on the existence of a line of thrust within the allowable zone permitted by the stress conditions. An example of how these conditions can be applied in a continuous beam with three different spans is given.

Notation

Position measured positive downwards from the centroid
Tensile stresses are positive
Sagging moments are positive

A	area
c_1	highest position of cable allowing for cover
c_2	lowest position of cable allowing for cover
d	permissible range of position of cable (allowing for cover)
e	eccentricity
e_m	eccentricity of line of thrust at mid-span
e_{max}	lower limit on eccentricity
e_{min}	upper limit on eccentricity
e_p	eccentricity of line of thrust
e_{pl}	eccentricity of line of thrust at left pier
e_{pr}	eccentricity of line of thrust at right pier
e_s	eccentricity of cable profile
E	Young's modulus
f_{ct}	permissible stress in compression at transfer
f_{cw}	permissible stress in compression at working load
f_{tt}	permissible stress in tension at transfer
f_{tw}	permissible stress in tension at working load
I	second moment of area about centroid
l_h	lever arm in hogging bending
l_s	lever arm in sagging bending
L	span
M_a	minimum working load moment
$(M_a)_{pl}$	M_a at left pier
$(M_a)_{pr}$	M_a at right pier
M_b	maximum working load moment
$(M_b)_m$	M_b at mid-span
M_f	moment range in one span (mid-span sagging - pier hogging)
M_{ls}	mean live load moment in one span
M_r	moment range at one section (sagging - hogging)

Written discussion closes 18 May 1988; for further details see p. ii.

* Imperial College of Science and Technology, London.

M_t moment at transfer
P_{max} maximum possible prestress at one section
P_{min} minimum possible prestress at one section
P_t prestressing force at transfer
P_1 minimum prestress to satisfy moment range
P_2 minimum prestress to satisfy lever arm
P_3 minimum prestress for existence of line of thrust
P_4 minimum prestress for existence of line of thrust and maximum cable range
Q_j secondary moment at internal support j
R (working load prestress)/(transfer prestress) ($= 1 -$ losses)
t_l linear transformation at left pier
t_m linear transformation at mid-span
t_r linear transformation at right pier
x position in span
y position in beam
y_1 position of top fibre (always $-$ve)
y_2 position of bottom fibre (always $+$ve)
$Z_1 = I/y_1$ (always $-$ve)
$Z_2 = I/y_2$ (always $+$ve)
β_j distribution coefficient for Q_j

Introduction

The design of continuous prestressed concrete bridges gives the engineer considerable freedom when compared with the design of statically determinate structures. By varying the secondary (or parasitic) moments, the relative magnitudes of the bending moments at mid-span and pier positions can be varied, thus allowing structures to be designed in which the line of thrust of the cable is outside the section, while the cable itself lies safely within the section.

2. The penalty to be paid for this freedom is greater complexity in design. It is necessary to determine the line of thrust of the actual cable that is used, or to choose a cable profile that is concordant. Either way, a knowledge and thorough understanding of the secondary moments in the structure are required.

3. Virtually all the standard texts on prestressed concrete design[1–3] dwell on the problems associated with the calculation of the line of thrust and secondary moments associated with a given cable profile, but do not consider in detail the wider implications for the designer. However, one Author has considered other aspects of the problem. Low[4,5] determined limits on the cable forces for the internal spans of a multi-span structure, based on considerations of potential crack patterns.

4. This Paper generalizes these ideas to include both the internal and end spans of a wider class of structures; those with unequal spans and those in which compressive stress limits govern.

Low's work

5. Low considered a typical internal span of a multi-span viaduct and distinguished four governing conditions which he expressed as limits on the minimum prestressing force within that span. These conditions were derived on the assumption that the beams were limited by tensile stresses, which can be visualized by potential crack patterns if the limits are exceeded (Fig. 1). The four cases can be summarized as follows.

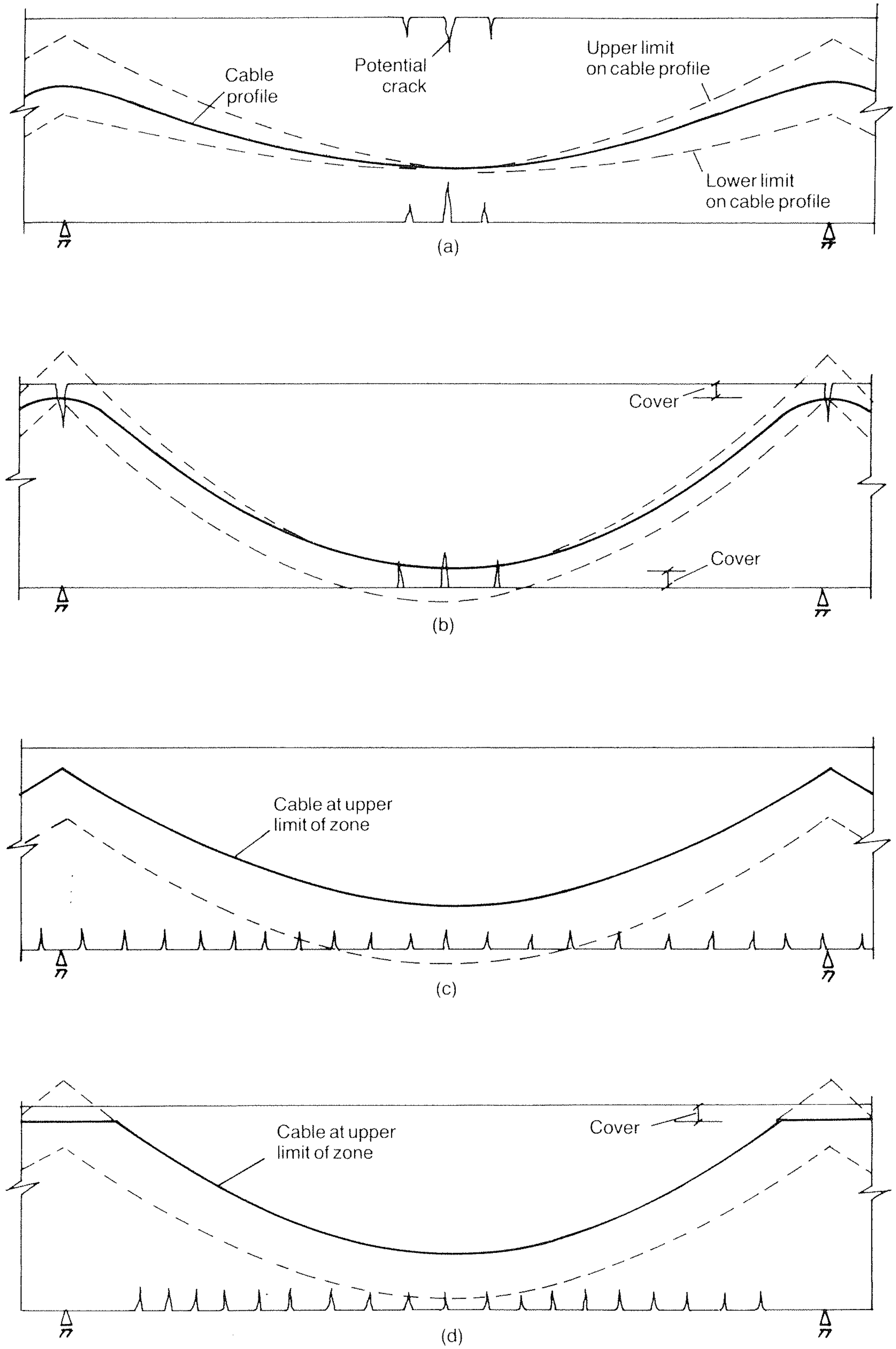

Fig. 1. Low's limits on cable forces (after reference 4): (a) limited by moment range (P_1); (b) limited by range of eccentricity (P_2); (c) limited by extension of extreme fibres (P_3); (d) as (c), but limited by cover over pier (P_4)

Case 1: governed by moment range

6. The beam cracks at the bottom under the maximum sagging load and at the top under the minimum sagging load, at the same section. The minimum prestressing force is shown to be a function of the live load moment range M_r, and is independent of the parasitic moment.

$$P_1 = \frac{M_r A}{(Z_1 - Z_2)} \tag{1}$$

Case 2: governed by lever arms

7. The beam cracks at the bottom at mid-span under the maximum moment and at the top over the piers under minimum moment. The limiting value of the minimum prestressing force is shown to be a function of the full moment range of the span M_f and the maximum lever arms within the section.

$$P_2 = \frac{M_f}{(l_s + l_h)} \tag{2}$$

It is implicit in this result that the parasitic moment has a specified value, in order to make maximum use of the section depth.

Case 3: governed by shortening of the extreme fibre

8. The span is assumed to be a typical internal span, so there must be no net rotation along the span caused by the prestressing force. The prestressing force is assumed to be sufficient just to eliminate the tensile stresses at all points in the bottom fibre owing to the average maximum live load moment M_{ls}. This leads to a limiting minimum prestressing force

$$P_3 = \frac{M_{ls} A}{Z_2} \tag{3}$$

One corollary of this result is that the cable is placed near the top of its allowable zone everywhere. Low demonstrates that this is often the governing condition for design.

Case 4

9. Case 4 is a special case derived on the same principles as case 3, but limited by the condition that the cable cannot be placed at the top of its allowable zone over the piers as this would fail to satisfy cover requirements. A more complicated limiting value for the prestressing force results, which need not concern us here.

10. Cases 1 and 2 are well established in practice and in texts, but case 3 was, as far as the Author can establish, novel. It was the desire to put case 3 on a more rigorous theoretical foundation which led to the work presented in this Paper. In order to establish common ground between the various cases, and 'conventional' views of prestressing, it is necessary to review, briefly, the main principles of section and cable design.

Magnel diagram and equations

11. The design of prestressed concrete beams at the working load is governed by stress criteria (see Appendix 1). These can be rearranged into eight inequalities

of the general form

$$e \geqslant -\frac{Z}{A} - \frac{Zf}{P} + \frac{M}{P} \tag{4}$$

These relationships form straight bound lines on a plot of e against $(1/P)$, a construction known as the Magnel diagram.[6] Each line passes through one of the Kern points ($e = -Z_1/A$ or $-Z_2/A$) when $1/P = 0$ ($P = \infty$). Therefore, four (and only four) of the inequalities define a feasible region which gives all valid combinations of force and eccentricity. Which four of the possible eight equations govern depends on the circumstances, but two will relate to the top fibre and two to the bottom fibre. Of each pair, one will be a tension limit and the other a compression limit.

12. The condition that the feasible region exists, which is an overriding condition in all cases (although not necessarily the governing one), is that the range of stresses in a particular fibre is less than the permissible stress range. These conditions can be expressed as limits on the elastic section moduli (Z_1 and Z_2). These inequalities are detailed in Appendix 1. It will be assumed henceforth that a section has been chosen already such that all these conditions are satisfied at all points along the length of the beam.

13. A typical Magnel diagram is shown in Fig. 2. The minimum and maximum

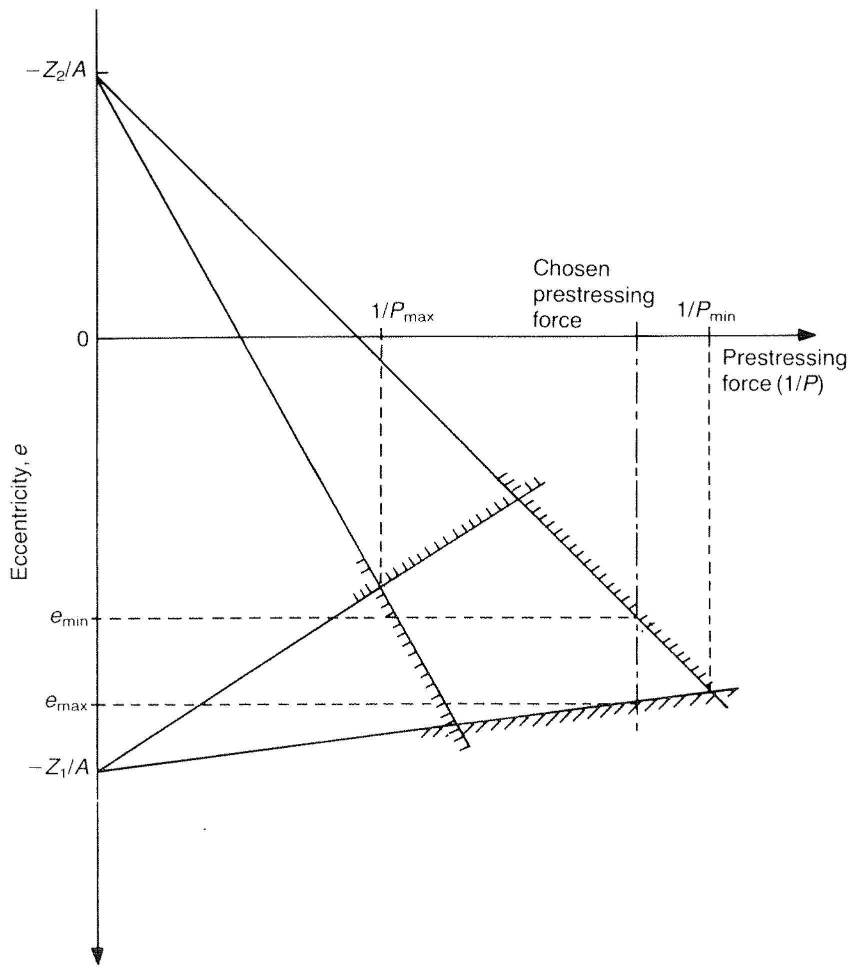

Fig. 2. Typical Magnel diagram

prestressing forces P_{min} and P_{max} can be identified. If the chosen prestressing force is close to P_{max}, then compressive stresses will govern, while if P is close to P_{min}, then tensile stress conditions will govern. Because minimizing the prestressing force usually results in greater economy, it will normally be found that a design is limited by tensile stresses.

14. However, if a section is chosen that only just satisfies the limiting conditions on the elastic modulus, a different result may be obtained. Suppose a road bridge is being considered, which will necessarily have a large top slab to carry the traffic. Local bending criteria will normally govern, so the section will have a top fibre modulus that is larger than required by the global flexural conditions. There is no reason why the bottom slab need be any larger than required to satisfy flexural criteria, so it is found that the Magnel diagram can look like that shown in Fig. 3.

15. The feasible region is long, but thin, and for most allowable prestressing forces is bounded by one tension limit and one compressive limit, even when P is

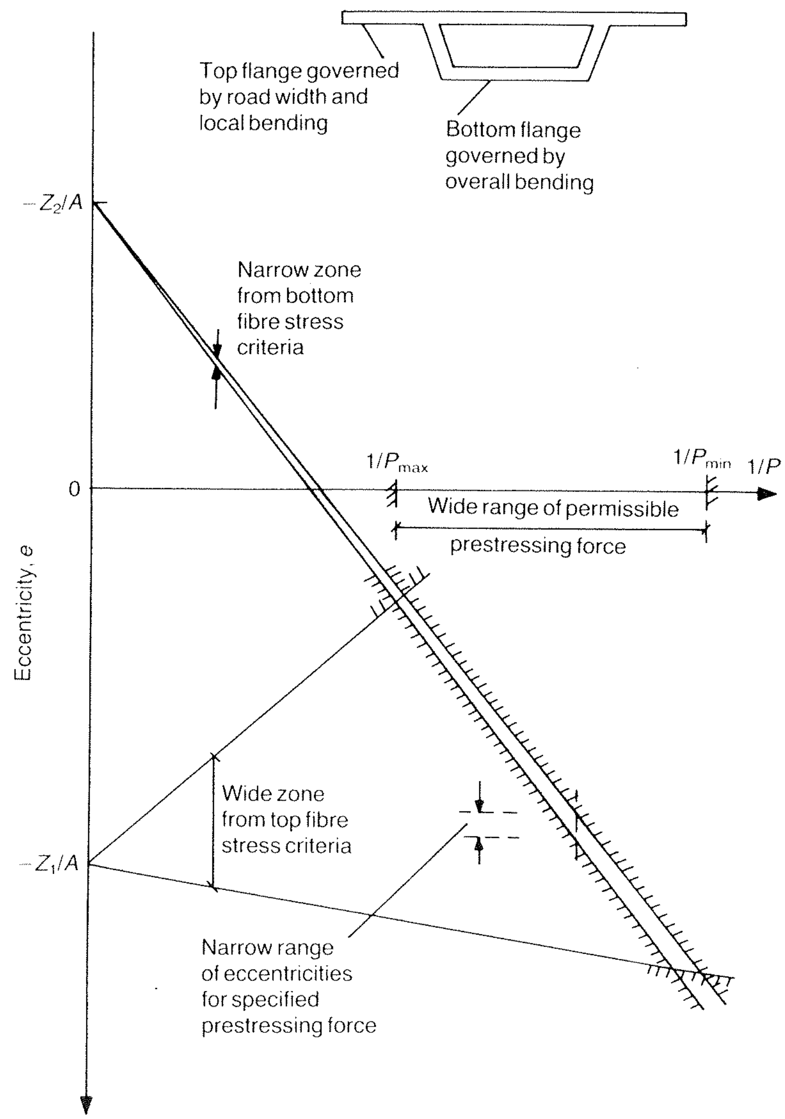

Fig. 3. Magnel diagram for a road bridge

close to P_{min}. A similar result obtains for trough beam railway bridges, in which the rails are mounted on the bottom slab, which therefore is large, and it is the top flange which can be kept small.

16. The applied moments vary along the length of the beam. We can thus calculate P_{min} and P_{max} at all positions along the length of the beam, and plot these as functions of position. P_{min} will be largest at mid-span and over the piers, which are the positions where the moment range is largest, so the feasible region of the Magnel diagram is smallest. Similarly, P_{max} will be smallest at these positions. If the tensile stress limits are put to zero, then P_{min} is identical to Low's value P_1.

Line of thrust design

17. The parasitic moments and their implication for design now need to be considered. Generally, any prestressing cable profile will induce flexural deflexions in the beam: if the beam is statically determinate, these cause no additional moments, as they are not resisted by the supports; if the beam is indeterminate, the tendency to deflect is resisted by the supports, whose reactions cause additional moments in the beam, known as secondary or parasitic moments M_2. However, because these moments are neither necessarily small (as implied by secondary) nor necessarily deleterious (as implied by parasitic), both terms are confusing.

18. If the actual position of the cable is given by e_s, it can be stated that the cable appears to act at its line of thrust e_p, where

$$Pe_p = Pe_s - M_2 \tag{5}$$

so that

$$e_p - e_s = -M_2/P \tag{6}$$

19. The calculation of M_2, and hence e_p, for a particular cable profile is straightforward. The forces that the cable exerts on the concrete can be calculated, and the response of the structure to these loads determined by a continuous beam program. This equivalent load method is well described in many texts (see, for example, reference 3).

20. Alternatively, and for our purposes, more conveniently, the secondary moments can be determined by considering the cable profile directly, using the principle of virtual work. The relevant equations are given in Appendix 2. The benefit for our purposes is that the method combines the structural analysis with the determination of the secondary moments, so we end up with a direct relationship between the cable profile and the secondary moments.

21. A few definitions will be required, but they are well known and are derived elsewhere.[7] If $M_2 = 0$, e_p and e_s coincide, and the profile is concordant. All e_p are themselves concordant profiles. Since M_2 is the result of a set of self-equilibrating support reactions, it varies linearly between supports; the difference $e_p - e_s$ will also vary linearly if the prestressing force is constant, must be zero at end supports, and is known as a linear transformation. Once e_p is known, any linear transformation will give a cable profile with the same line of thrust.

22. Two design philosophies can be identified, but they are equivalent.

(*a*) If the secondary moments are considered as prestressing effects, the stress conditions which lead to the Magnel diagram give limits on e_p. For any chosen prestressing force, these can be plotted along the length of the beam; the designer has to find a concordant profile that satisfies these limits. A suitable linear transformation can be determined to find a practical cable profile that satisfies cover requirements.

(*b*) If the designer has some estimate of the secondary moments, they can be regarded as loads, and included in the moments from which the Magnel diagram is calculated. The eccentricity limits are thus limits on e_s, and the problem becomes one of finding an actual cable profile which satisfies these conditions and causes the assumed secondary moments.

In practice, the choice between these methods is one of personal preference; the present Author finds the first easier, but knows many engineers who claim that they do not 'bother about concordant profiles', yet still correctly deal with secondary moments and indeed use them to considerable advantage.

23. For present purposes the first method will be used, as it requires no *a priori* knowledge of the secondary moments. The eccentricity inequalities (equations (25)–(32)) will be used to produce envelopes of the permissible line of thrust. The upper limit on the cable position will be termed e_{min} and the lower limit e_{max}. These limits may be governed by different conditions at different positions along the beam, and will be functions of the chosen prestressing force.

Design for limiting eccentricity

24. For any particular structure, with specified spans and loading, limits on the line of thrust e_p can be determined. A typical allowable zone will look like that shown in Fig. 4. The line of thrust will be high over the piers, and low at mid-span, as would be expected.

25. The effect of applying a linear transformation to the limiting values of e_p can now be considered. If a sagging secondary moment is chosen, the effect will be to produce a cable profile e_s which is lower than e_p. This can be an advantage: cover requirements for e_s have to be satisfied, but not for e_p. Therefore, it does not matter if the line of thrust lies outside the section over the piers, provided that the corresponding cable is within the section.

26. What range of secondary moments is permissible? In the case of the e_p

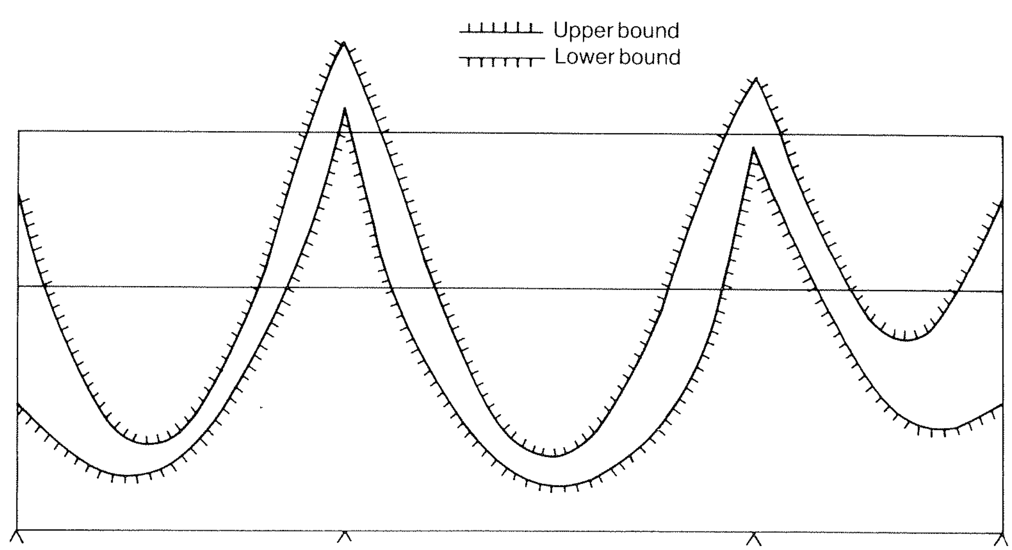

Fig. 4. Typical limits on line of thrust

limits shown in Fig. 4, the secondary moments must be large enough to bring the cable into the section (and allow for cover) over the piers, but not so large that the cable loses cover at the bottom at mid-span. Bearing in mind that the form of the secondary moment variation is known along the beam, in that it is zero at pinned ends and varies linearly between supports, there is either an infinity of possible solutions, a unique solution or no solution. The condition that there is a unique solution needs to be determined, as this represents the dividing line between a feasible and an unfeasible design.

27. Consider the single internal span shown in Fig. 5(a). The existence of symmetry will not be assumed for the moment. A positive linear transformation is required at both pier positions, to bring the cable within the allowed zone, but a larger value is required at the left-hand pier. However, the linear transformation must not be too large near mid-span. The two limits are shown in Fig. 5(b) as functions of position within the span. The difference $e_p - e_s$ varies linearly along the span, and, as drawn, many possible lines can be fitted between the bounds. The condition that one line can just be fitted between the bounds on the transformation is being sought. This will occur when a point on the upper bound is just tangential to the line joining the two values over the piers, as shown in Fig. 5(c).

28. Let the position within the span where the transformation is tangential be at a distance of x from the left-hand end. Then

$$t_m \geqslant \frac{x}{L} t_r + \frac{(L-x)}{L} t_l \tag{7}$$

and

$$\begin{aligned} t_r &= c_1 - e_{pr} \\ t_l &= c_1 - e_{pl} \\ t_m &= c_2 - e_m \end{aligned} \tag{8}$$

which can be rearranged to give

$$d \geqslant e_m - e_{pr} \frac{x}{L} - e_{pl} \frac{(L-x)}{L} \tag{9}$$

29. In any particular design, the stress conditions which govern at each section will be known; as there are four possibilities for each of e_m, e_{pr} and e_{pl}, there are 64 different combinations, so it is not sensible to detail all of them here. However, we can consider one case as an illustrative example.

30. If it is assumed that the working load conditions govern at each point, this gives

$$\begin{aligned} e_{pl} &= -\frac{Z_1}{A} - \frac{Z_1 f_{tw}}{RP_t} + \frac{(M_a)_{pl}}{RP_t} \\ e_{pr} &= -\frac{Z_1}{A} - \frac{Z_1 f_{tw}}{RP_t} + \frac{(M_a)_{pr}}{RP_t} \\ e_m &= -\frac{Z_2}{A} - \frac{Z_2 f_{tw}}{RP_t} + \frac{(M_b)_m}{RP_t} \end{aligned} \tag{10}$$

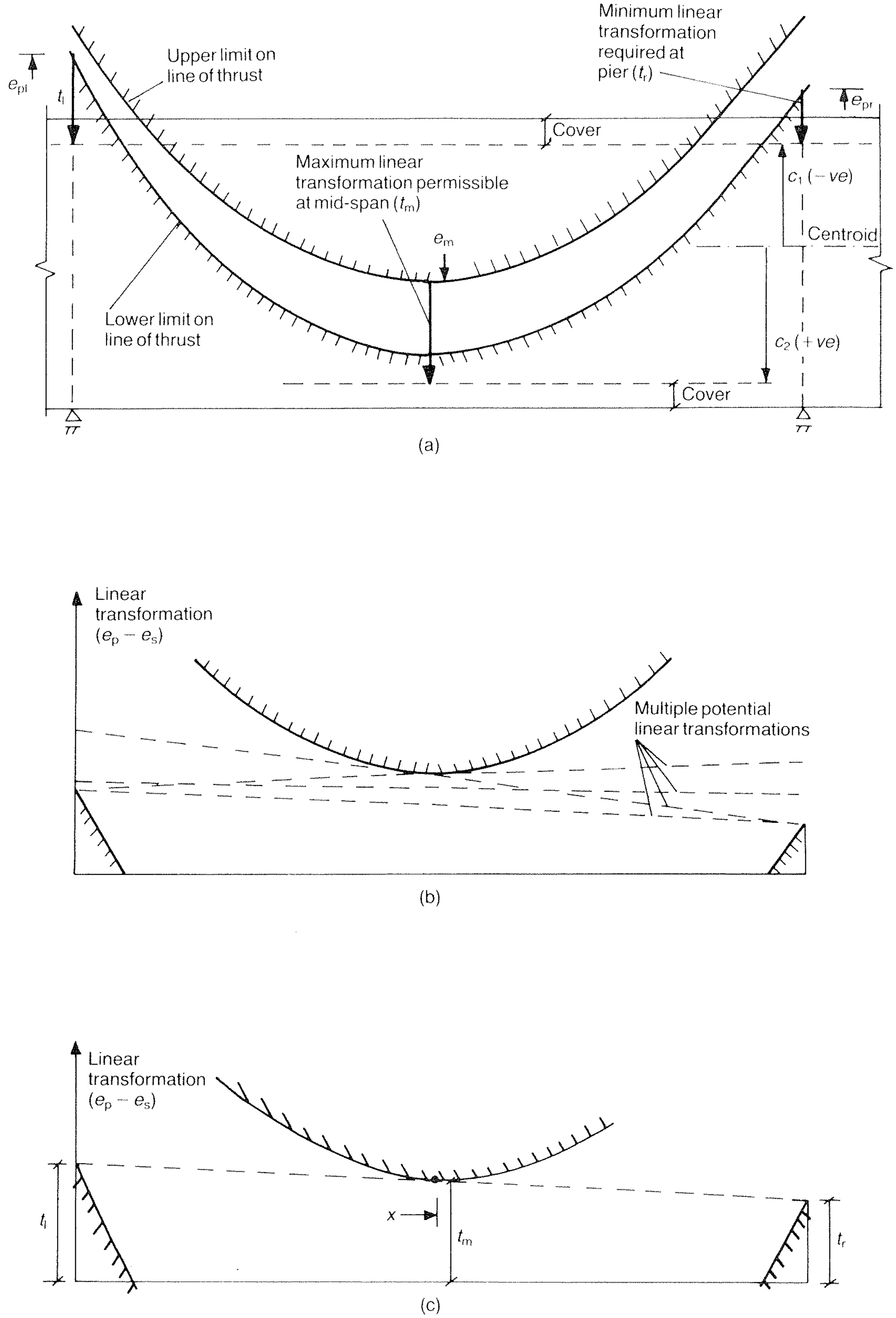

Fig. 5. Linear transformation for internal span: (a) typical internal span (L); (b) permissible linear transformations—general case; (c) permissible linear transformation—limiting case

Substituting into equation (9) and rearranging, gives

$$RP_t \geqslant \frac{\left[\left((M_b)_m - \frac{x}{L}(M_a)_{pr} - \frac{(L-x)}{L}(M_a)_{pl}\right) - f_{tw}(Z_2 - Z_1)\right]}{\left(d + \frac{(Z_2 - Z_1)}{A}\right)} \tag{11}$$

If the effects of losses are ignored, $f_{tw} = 0$, and the beam is symmetrical, so that $(M_a)_{pr} = (M_a)_{pl}$ and $x = 0{\cdot}5$, equation (11) reduces to Low's much simpler expression for P_2.

31. In an end span (say at the left-hand end of the beam), t_l must be zero.

$$t_m \geqslant (x/L)t_r \tag{12}$$

so that

$$e_m \geqslant \left(c_2 - \frac{x}{L}c_1\right) + \frac{x}{L}e_{pr} \tag{13}$$

which leads to

$$RP_t \geqslant \frac{\left[\left((M_b)_m - \frac{x}{L}(M_a)_{pr}\right) - f_{tw}\left(Z_2 - \frac{x}{L}Z_1\right)\right]}{\left[\left(c_2 - \frac{x}{L}c_1\right) + \frac{(Z_2 - (x/L)Z_1)}{A}\right]} \tag{14}$$

A similar result can be derived for right-hand end spans.

32. In general in internal spans, and in all cases in end spans, the value of x is unknown. However, it is easy to determine which stress condition governs the position of the line of thrust at the piers, and also at intermediate positions, and to produce similar equations in all cases.

33. It should be appreciated that these results are a relaxation of the conditions that apply for statically determinate beams, in which secondary moments cannot occur; the limits on cover must be applied at every section to the line of thrust of the cable, which now coincides with the actual position.

Conditions on existence of line of thrust

34. Consideration has not yet been given to the question of whether it is actually possible to find a line of thrust e_p which satisfies the stress limits. In the general case, the line of thrust will be constrained to lie between bounds e_{min} and e_{max} defined by the various forms of equation (25). Typically, the bounds will rise over piers but will lie below the centroid in regions where the bending moments are sagging. Provided that the prestressing force has been chosen so that it lies within the feasible region of the Magnel diagram for all positions along the beam, it follows that $e_{max} \geqslant e_{min}$ for all positions.

35. A cable placed at the lowest position e_{max} will cause the maximum possible sagging secondary moments $M_{2\,max}$. (Imagine that the beam is made statically determinate by the removal of the internal supports. The effect of the cable's acting alone will be to induce the maximum hogging curvature in the beam and hence the

largest uplift at the intermediate support positions. It will then require the largest downward forces at the intermediate positions to restore the beam to its undeflected position at the supports, thus maximizing M_2.)

36. For normal beams, subjected to gravity loads applied within the length of the beam, the resulting bending moment diagram will normally have larger sagging regions than hogging regions, so the corresponding secondary moments are normally sagging.

37. By a similar argument, a cable placed at e_{min} will cause the maximum hogging (or minimum sagging) secondary moment ($M_{2\ min}$). If the maximum and minimum secondary moments are both sagging, it follows that it will be impossible to find an intermediate cable profile that causes zero secondary moments; no line of thrust can thus exist.

38. This is the essence of Low's third condition on the prestressing force P_3. If the prestressing force is too low, no concordant line of thrust will be found to exist; a search for it would be fruitless. Low's condition is based on the assumption that there must be sufficient prestress to ensure that the bottom fibre does not decompress, and that the total shortening of the bottom fibre due to the prestress is the same as the shortening of the centroid. There will thus be no net rotation along the span which is necessary to allow multiple spans all to have the same structural form and cable layout. More simply, this is a compatibility condition to ensure that individual spans in the viaduct fit together.

39. The condition for concordancy of the line of thrust is a similar compatibility condition, although usually expressed in terms of displacement rather than slope, at the supports. Despite that difference, they are the same condition in practice. The present condition is more general. It applies to the whole structure, including end spans, and can take account of the fact that different stress conditions apply at different positions along the beam.

40. There are expressions for e_{min} and e_{max} at all positions along the length of the beam, from equations (25)–(32) and for any chosen prestressing force, the secondary moments at each pier position can be determined, using equations (47). It is thus straightforward in the design process to try various prestressing forces until the maximum and minimum secondary moments at each pier position are of opposite signs, indicating that a concordant line of thrust exists and can be sought.

41. However, it would be beneficial to be able to find conditions which must be satisfied to enable us to find the minimum prestressing force directly. $M_{2\ max}$ will normally be sagging in all cases, but $M_{2\ min}$ can be sagging or hogging. Therefore, the dividing line between these two cases, which will occur when e_{min} itself defines a concordant profile, has to be found. Can any condition which must be satisfied for e_p to exist be determined?

42. Consider equation (47) which defined the secondary moments Q_j at each internal support. If the cable profile is concordant, then all Q_j are zero. It is both a necessary and a sufficient condition for this result that the right-hand sides are all, separately, zero. Thus it can be shown that a cable profile is concordant if it can be shown that

$$\int \frac{\beta_i Pe \, dx}{EI} = 0 \quad \text{for all i} \tag{15}$$

This result is perfectly general, although not particularly useful in its present form.

43. If it is assumed that both EI and P are constant everywhere, then it is only

necessary to show that

$$\int \beta_i e \, dx = 0 \quad \text{for all } i \tag{16}$$

Although these integrals are formally for the complete structure, in practice, for any i, the β_i values are only non-zero in the spans adjacent to the ith support. A sufficient (but not necessary) condition to ensure concordancy of e is that $\int \beta_i e \, dx$ is zero for each span separately.

44. Consider a beam whose internal spans are of roughly equal size and whose end spans are so proportioned that the maximum hogging moments over all supports are approximately the same. This is a common layout for multi-span structures, although there are many exceptions.

45. For internal spans it is common practice to make the cable profiles identical within each span, and symmetric about the mid-span. β_i is skew-symmetric about the mid span, where it takes the value 0·5. Thus $\int \beta_i e \, dx = 0{\cdot}5 \int e \, dx$, so we only need to show that the average value of the eccentricity is zero within the span.

46. It is usual, although again not invariable, that the value of e_{min} will be governed by the tensile stress limit in the bottom fibre under the action of the maximum moment M_{b}. Therefore, e will satisfy identically the condition that

$$e = -\frac{Z_2}{A} - \frac{Z_2 f_{\text{tw}}}{RP_{\text{t}}} + \frac{M_{\text{b}}}{RP_{\text{t}}} \tag{17}$$

Thus, if $\int e \, dx = 0$

$$L\left(-\frac{Z_2}{A} - \frac{Z_2 f_{\text{tw}}}{RP_{\text{t}}}\right) + \frac{1}{RP_{\text{t}}} \int M_{\text{b}} \, dx = 0 \tag{18}$$

where L is the span.

47. If the average value of M_{b} over the span is $\bar{M}_{\text{b}}$, then the condition can be rearranged to give

$$RP_{\text{t}} = \frac{\bar{M}_{\text{b}} - Z_2 f_{\text{tw}}}{Z_2/A} \tag{19}$$

It is relatively easy to show that this is a minimum condition on the prestressing force. If P_{t} is less than this value, e_{min} will give rise to a sagging secondary moment, and no concordant profile can exist.

48. This expression is a general form of Low's limit on P_3. Low set f_{tw} to zero, and his expression uses the mean value of the maximum live load moment, whereas the Author's expression uses the mean value of the maximum total moment. However, he postulates a beam in which, owing to dead load, no rotation occurs over the piers; in that case, the mean value of the dead load moment will also be zero.

49. For end spans, slightly different conditions apply, as the results cannot be simplified by symmetry. Consider the first span, where we only need to show that $\int \beta_1 e \, dx = 0$. If we measure distance x from the end of the beam, up to the first support at $x = L$, then $\beta_1 = x/L$. If e_{min} is governed by the same stress condition as in the internal spans, then it needs to be shown that

$$\int_0^L \frac{x}{L}\left[\left(-\frac{Z_2}{A} - \frac{Z_2 f_{\text{tw}}}{RP_{\text{t}}}\right) + \frac{M_{\text{b}}}{RP_{\text{t}}}\right] dx = 0 \tag{20}$$

or

$$-L\left(\frac{Z_2}{A}+\frac{Z_2 f_{tw}}{RP_t}\right)+\frac{1}{RP_t}\int_0^L \frac{x}{L} M_b \, dx = 0 \tag{21}$$

Integrating by parts, gives

$$L\left(\frac{Z_2}{A}+\frac{Z_2 f_{tw}}{RP_t}\right)=\bar{M}_b L-\frac{1}{L}\int_0^L\left(\int_0^x M_b \, ds\right) dx \tag{22}$$

Defining

$$\tilde{M}_b \text{ as } \frac{1}{L^2}\int_0^L\left(\int_0^x M_b \, ds\right) dx \tag{23}$$

this equation can be rearranged to give

$$RP_t=\frac{\bar{M}_b-\tilde{M}_b-Z_2 f_{tw}}{Z_2/A} \tag{24}$$

50. These conditions are generalized forms of those given by Low, and although they only apply precisely in certain circumstances, they are a useful guide to the minimum prestress required. The average values of M_b within each span and the double integral of M_b in the end spans are easy to carry out numerically, and it is therefore straightforward to include these conditions in the design process.

Condition P_4

51. The condition that Low calls P_4 is a combination of the two cases P_2 and P_3. The limit which governs P_3 is that e_{min} is a concordant profile, and so may be a line of thrust. Such a profile will have a larger range than that given if the line of thrust passes through e_{max} over the piers, so it may not be possible to fit a cable into the section.

52. Therefore, it is necessary to find the condition that a cable with the lowest permissible range of eccentricities will be a concordant profile. Low got round this by assuming that the actual cable profile was at its maximum practical negative eccentricity (i.e. c_1) over the piers, and remained at that eccentricity until forced down by the conditions on emin. This is slightly artificial in that the cable will have to be curved in practice, but the principle is valid, and will not be dealt with in detail here.

Visualization of conditions

53. The four conditions that have been discussed can be summarized by visualizing the allowable limits on e_p.

- P_1 The conditions on P_1 ensure that a feasible zone for e_p exists, so that $e_{max} > e_{min}$ (Fig. 6(a)).
- P_2 The condition P_2 ensures that the range of eccentricities within a span are less than allowable by considerations of cover (Fig. 6(b)).
- P_3 The condition P_3 ensures that a concordant profile exists between the limits e_{min} and e_{max} (Fig. 6(c)).

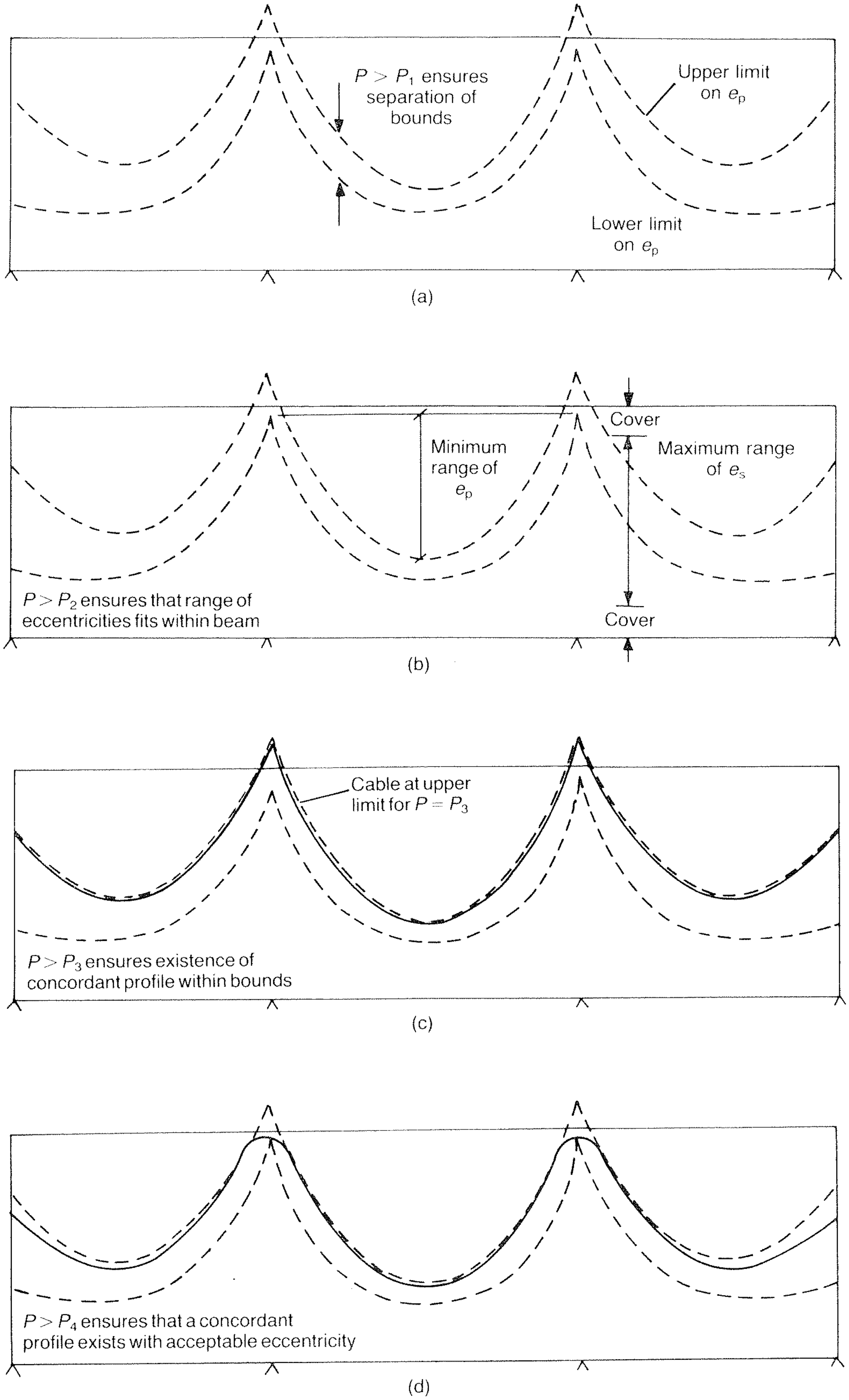

Fig. 6. Visualization of limiting force conditions: (a) P_1; (b) P_2; (c) P_3; (d) P_4

P_4 The condition P_4 ensures that a cable which satisfies the eccentricity range condition (as for P_2) will also satisfy the condition that a concordant line of thrust can exist (as for P_3) (Fig. 6(d)).

Example

54. As an illustration of some of the principles discussed previously, the design of a 3-span bridge, with spans of 40 m, 50 m and 30 m, will be considered. The structure is to carry three traffic lanes, each 3·65 m wide within an overall width of 13 m.

55. The loading is to be standard highway loading HA plus 45 units of HB, to the Department of Transport draft standard.[8] The concrete will be assumed to have permissible stresses in compression of -15 N/mm^2 at transfer and of $-16{\cdot}5$ N/mm^2 at the working load (tensile stresses are considered positive), with no tension being allowed in the preliminary design. The section will be prismatic. The live load envelopes are determined using an enveloping program based on Macauley's method[9] (Fig. 7).

56. The largest moment ranges occur at the centre of left-hand side span (chainage 20 m—moment range 37 040 kNm), and over the left-hand pier (chainage 40 m—moment range 28 193 kNm). These will thus be regarded as the critical positions for the section design.

57. The section design is based on the moment range at the critical sections, which leads to minimum section moduli of $-2{\cdot}24$ m^3 for Z_1 and $2{\cdot}64$ m^3 for Z_2. The chosen section is shown in Fig. 8; the overall depth is chosen from span : depth ratio considerations, while the top flange is fixed by the road width and is considerably larger than that required for purely flexural considerations. The bottom flange is only marginally above the minimum size.

58. Figure 9 shows the Magnel diagrams at the two critical positions (20 m

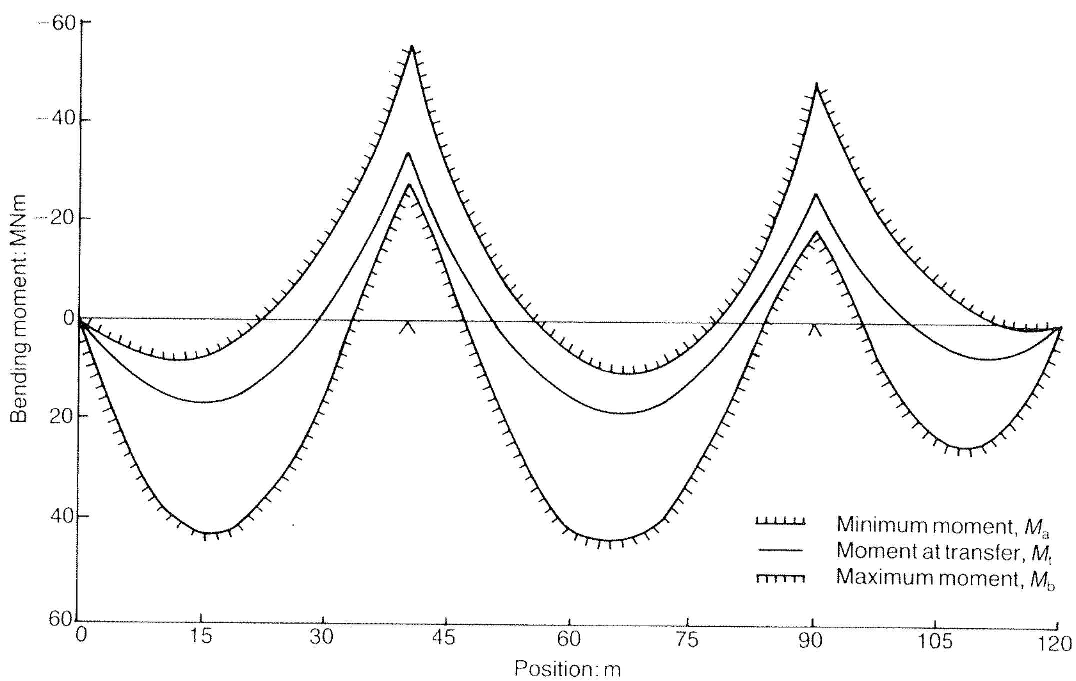

Fig. 7. Moment envelopes used in design example

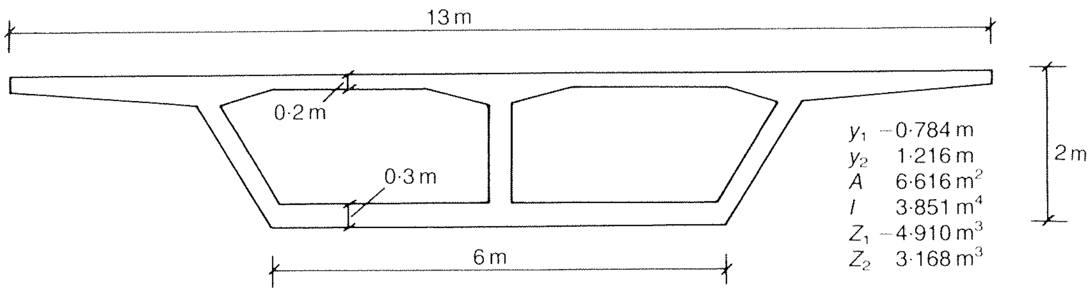

Fig. 8. Cross-section chosen for design example

and 40 m). The minimum prestressing forces at the two sections are 40 449 kN and 33 538 kN respectively. The feasible region lies outside the section at the top at chainage 40 m, but the feasible region lies well within the section at 20 m, so it is probable that the cable can be brought within the section when linear transformations and the associated secondary moments are considered.

59. The requisite prestress force can now be considered. The first criterion is that a feasible region must exist on the Magnel diagram at each cross-section (P_1).

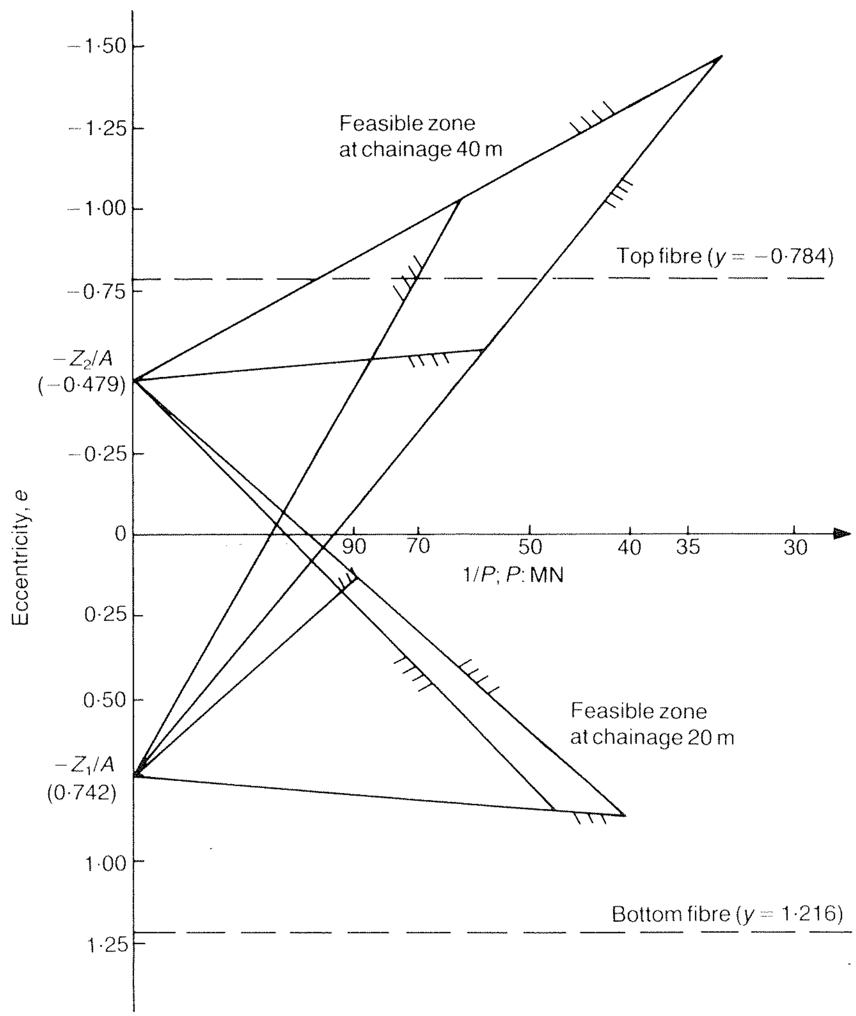

Fig. 9. Magnel diagrams at 20 m and 40 m from left-hand end

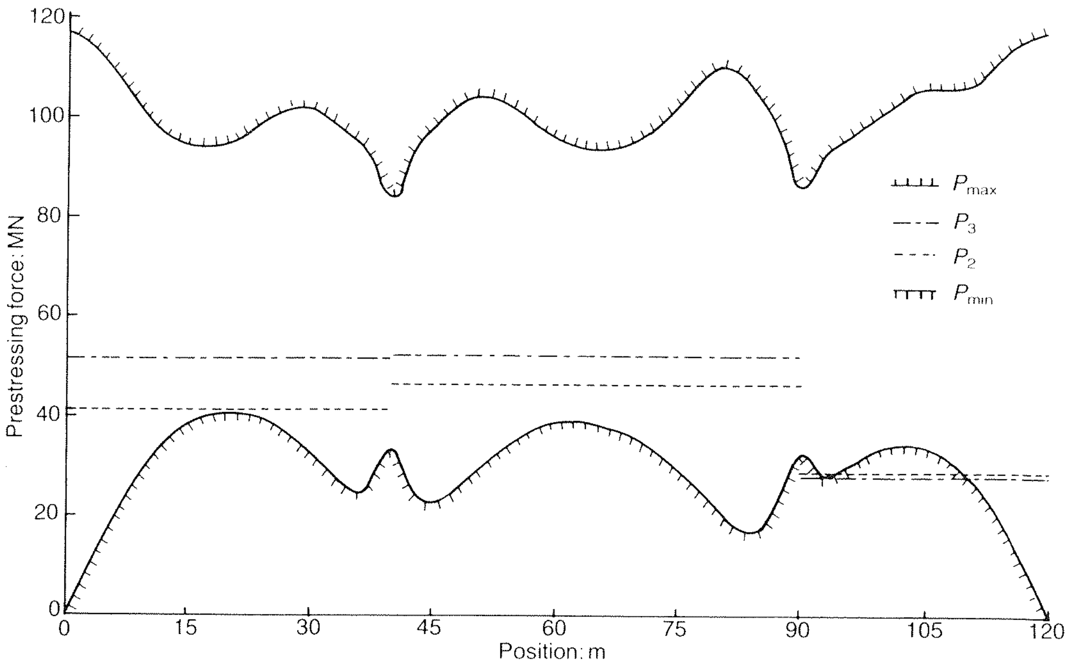

Fig. 10. Limits on prestressing force

The minimum and maximum prestressing forces (calculated by the standard elastic design inequalities (25)–(44) given in Appendix 1) are shown in Fig. 10. The maximum force is unlikely to be a governing criterion, but the minimum prestressing force must be at least 40 449 kN. However, the other two criteria must also be checked.

60. The values for P_2 calculated on the basis of the eccentricity range are

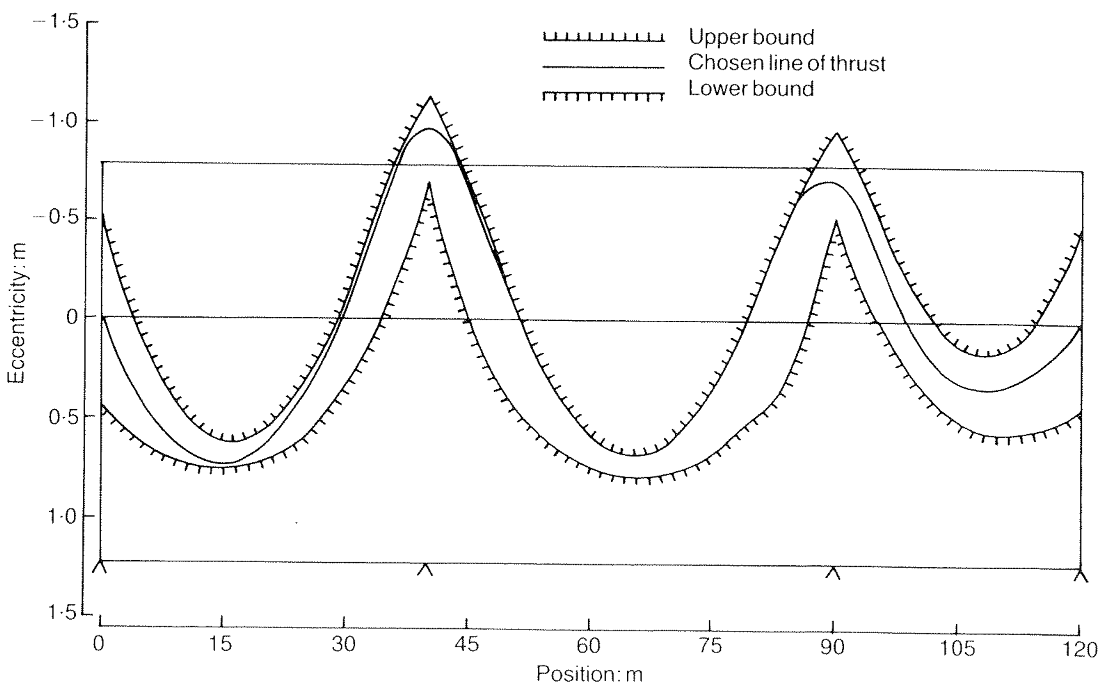

Fig. 11. Limits on line of thrust of cable e_p

Table 1. Values for P_2 and P_3

Span	P_2 : kN	P_3 : kN
Left	41 172	51 438
Centre	46 137	51 822
Right	28 520	27 731

shown in Table 1, as are those calculated for P_3 on the assumption that a concordant profile exists within the line of thrust zone. Clearly, a prestressing force of at least 51 822 kN is required. If a prestressing force of 52 000 kN is chosen, inequalities (25)–(32) can be used to determine limits on the line of thrust e_p which are shown in Fig. 11.

61. As a check on the existence of a concordant profile, the secondary moments, that result if a cable at the highest position e_{min} and the lowest position e_{max} is chosen, can be calculated (see Table 2). Clearly, it is possible to find a concordant cable profile which fits within these limits, but we would expect it to lie close to the upper limit on e_p, especially in the left and centre spans.

62. A line of thrust can be sought which satisfies the limits on e_p. Use will be made of the principle that any bending moment diagram which corresponds to a real load on the structure will be a scaled line of thrust. A notional cable force of 1000 kN will be assumed, so that a bending moment of 1000 kNm corresponds to an eccentricity of 1 m; and a continuous beam program will be used to calculate the results.

63. The process is iterative, and takes several steps; a load is assumed, the bending moments calculated, and they are compared with the eccentricity limits. If the calculated eccentricity lies outside the limits, a modification to the applied loads is made, and the process repeated. The loads are also chosen to minimize the reaction at the internal supports, to eliminate kinks in the cables at these points. An automated version of this process will be presented separately.[10]

64. The first estimate was to take a uniformly distributed load over the whole structure, of intensity 7 kN/m. After a number of iterations, the loading was modified to have 8 components (see Table 3). The corresponding line of thrust is shown in Fig. 11. As expected, the cable profile is close to the upper limit over the main span, and for a fair proportion of the left-hand span.

65. The profile lies above the beam at the left-hand pier, but is well above the soffit at mid-span. A linear transformation can now be used to choose a cable profile that fits within the section. The cable profile needs to be lower than the line of thrust by 0·334 m at the left pier, and 0·079 m at the right pier, to give 0·15 m from the top surface to the centre of the cable. With a cable force of 52 000 kN, this

Table 2. Secondary moments at internal supports

	Q_1 : kNm Left pier	Q_2 : kNm Right pier
e_{min} (hogging)	−315	−3384
e_{max} (sagging)	16 029	15 941

Table 3. Notational loading to give e_p

Load	Start	End	Intensity: kNm
1	0·0	30·0	6·8
2	30·0	35·0	5·0
3	35·0	45·0	−25·6
4	45·0	55·0	5·2
5	55·0	82·5	7·0
6	82·5	95·0	−18·8
7	95·0	105·0	10·0
8	105·0	120·0	5·0

corresponds to secondary moments of 17 368 kNm and 4108 kNm (before losses), at these positions.

66. To demonstrate that the limits on the actual cable zone e_s are also satisfied, these secondary moments can be treated as loads, and the limits determined. These are shown in Fig. 12, together with the actual cable profile, and it can be seen that the conditions are satisfied. (It must be stated that this check is academic—if the limits on e_p are satisfied, then those on e_s will automatically be satisfied.)

Conclusion

67. It has been shown that a constraint on the existence of a feasible line of thrust, within the zone permitted by the stress criteria, must be considered when choosing the prestressing force in a statically indeterminate beam.

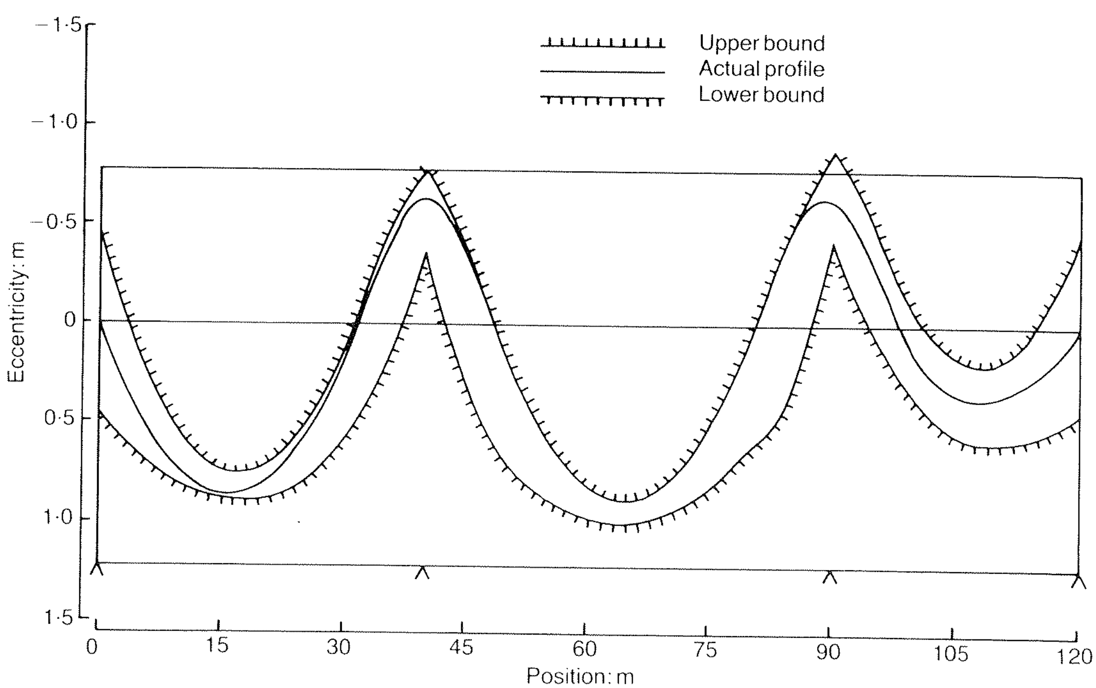

Fig. 12. Limits on actual cable profile e_s

68. This condition has been shown to be a generalization of Low's condition on the extension of the extreme fibre.

69. An example has been given demonstrating the use of this condition in practice, and illustrating the steps needed to design cable profile rationally and quickly.

Appendix 1. Stress limit criteria

70. At any cross-section, the beam will be loaded by a minimum working load moment M_a and maximum moment M_b, which are applied after all prestressing losses. Before time dependent losses have occurred, it will be assumed that there is a fixed transfer moment M_t. If the stresses are limited to f_{tt} in tension and f_{ct} in compression at transfer, and f_{tw} in tension and f_{cw} in compresssion at the working load, 12 distinct stress criteria can be identified, based on limiting tension and compression in both extreme fibres under the three load conditions. However, if it is insisted that $M_b \geqslant M_a$, this number can be reduced to eight, as four will automatically be satisfied.

71. These conditions can be rearranged to give inequalities on the permissible eccentricities, as functions of the applied moments, the section properties and the reciprocal of the prestressing force.

$$e \geqslant -\frac{Z_1}{A} - \frac{Z_1 f_{ct}}{P_t} + \frac{M_t}{P_t} \tag{25}$$

$$e \geqslant -\frac{Z_1}{A} - \frac{Z_1 f_{cw}}{RP_t} + \frac{M_b}{RP_t} \tag{26}$$

$$e \geqslant -\frac{Z_2}{A} - \frac{Z_2 f_{tt}}{P_t} + \frac{M_t}{P_t} \tag{27}$$

$$e \geqslant -\frac{Z_2}{A} - \frac{Z_2 f_{tw}}{RP_t} + \frac{M_b}{RP_t} \tag{28}$$

$$e \leqslant -\frac{Z_1}{A} - \frac{Z_1 f_{tt}}{P_t} + \frac{M_t}{P_t} \tag{29}$$

$$e \leqslant -\frac{Z_1}{A} - \frac{Z_1 f_{tw}}{RP_t} + \frac{M_a}{RP_t} \tag{30}$$

$$e \leqslant -\frac{Z_2}{A} - \frac{Z_2 f_{ct}}{P_t} + \frac{M_t}{P_t} \tag{31}$$

$$e \leqslant -\frac{Z_2}{A} - \frac{Z_2 f_{cw}}{RP_t} + \frac{M_a}{RP_t} \tag{32}$$

72. By considering the change in stress in a particular fibre, and comparing it with the permissible stress range, three limiting conditions for the elastic section modulus of each extreme fibre can be derived.

$$Z_1 \leqslant -\frac{(M_a - RM_t)}{(Rf_{ct} - f_{tw})} \tag{33}$$

$$Z_1 \leqslant \frac{(M_b - RM_t)}{(f_{cw} - Rf_{tt})} \tag{34}$$

$$Z_1 \leqslant \frac{(M_b - M_a)}{(f_{cw} - f_{tw})} \tag{35}$$

$$Z_2 \geqslant -\frac{(M_b - RM_t)}{(Rf_{ct} - f_{tw})} \tag{36}$$

$$Z_2 \geqslant \frac{(M_a - RM_t)}{(f_{cw} - Rf_{tt})} \tag{37}$$

$$Z_2 \geqslant \frac{(M_a - M_b)}{(f_{cw} - f_{tw})} \tag{38}$$

73. Once a section has been chosen, a Magnel diagram can be drawn at the cross-section, and the maximum and minimum prestressing forces can be determined. Alternatively, by considering all combinations of top and bottom fibre stress limits, the following limits on the prestressing force can be derived.

$$P_t \geqslant -\frac{Af_{tw}}{R} + \frac{A}{R(Z_2 - Z_1)}(M_b - M_a) \tag{39}$$

$$P_t \geqslant \frac{A}{R(Z_2 - Z_1)}[(Rf_{tt}Z_1 - f_{tw}Z_2) + (M_b - RM_t)] \tag{40}$$

$$P_t \geqslant \frac{A}{R(Z_2 - Z_1)}[(f_{tw}Z_1 - Rf_{tt}Z_2) + (RM_t - M_a)] \tag{41}$$

and

$$P_t \leqslant -\frac{Af_{cw}}{R} - \frac{A}{R(Z_2 - Z_1)}(M_b - M_a) \tag{42}$$

$$P_t \leqslant \frac{A}{R(Z_2 - Z_1)}[(Rf_{ct}Z_1 - f_{cw}Z_2) - (RM_t - M_a)] \tag{43}$$

$$P_t \leqslant \frac{A}{R(Z_2 - Z_1)}[(f_{cw}Z_1 - Rf_{ct}Z_2) - (M_b - RM_t)] \tag{44}$$

These inequalities have been used in the Paper to provide upper and lower limits on the prestressing force P_{min} and P_{max}.

Appendix 2. Calculation of secondary moments by virtual work

74. It is possible to determine the secondary moments on a beam directly from the cable profile, using the principle of virtual work. It is still necessary to solve a set of simultaneous equations (one for each internal support), but it is not necessary to convert the cable profile into the equivalent forces and then perform a structural analysis.

75. An equilibrium system consisting of a *fictitious* moment system and associated reactions, as shown in Fig. 13(a), is identified. The reactions R'_{ik} are unknown but will not need to be determined. There will be one such equilibrium system for every internal support.

76. The compatibility system will be chosen to be the *actual* displacement of the beam. There will be a curvature (+ve sagging) due to the horizontal component of the prestressing force (P) at an eccentricity (e) of $-Pe/EI$. The $-$ve sign arises because a cable with +ve eccentricity causes a hogging curvature.

77. At each internal support there will be an actual secondary moment Q_j, as shown in Fig. 13(b). Each of these secondary moments will give rise to a curvature of $\beta_j Q_j/EI$, which varies along the length of the beam.

78. The virtual work equation will thus be

$$\int_0^L M\kappa \, dx = \sum W\Delta \tag{45}$$

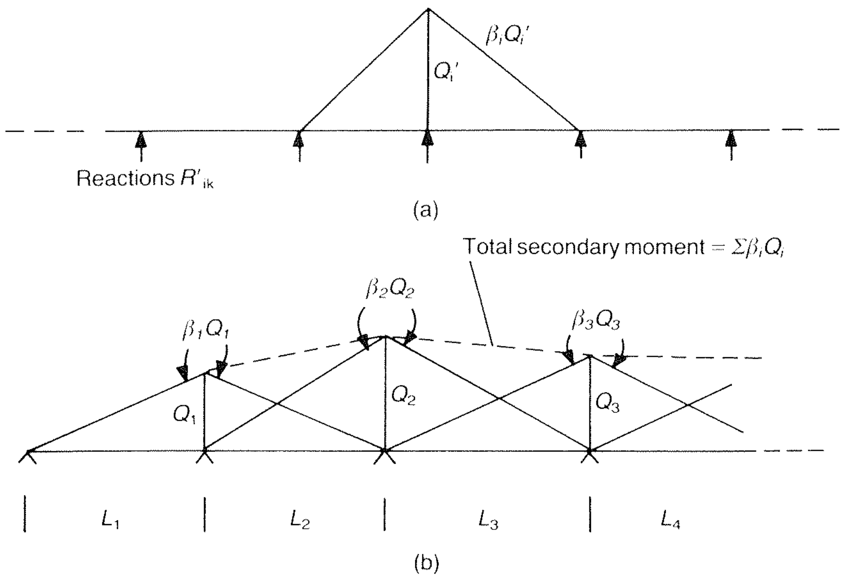

Fig. 13. Virtual work systems: (a) equilibrium system; (b) compatibility system

79. The only point forces on the beam in the equilibrium system are the reactions R'_{ik}, but as these are applied at the supports, where Δ is zero, then the right-hand side of the virtual work equation must be zero and we do not need to know the values of R'_{ik}.

80. There will thus be one virtual work equation for each of the internal supports.

$$\int \beta_i Q_i'\left(\sum_j \beta_j Q_j - Pe\right)/EI \, dx = 0 \qquad i = 1, 2, \dots n \qquad (46)$$

81. For any particular equation, Q_i' is a constant, so it can be cancelled from the equation without loss of generality, which can be rearranged to give

$$\sum_j Q_j \int \frac{\beta_i \beta_j \, dx}{EI} = \int \frac{\beta_i Pe \, dx}{EI} \qquad i = 1, 2, \dots n \qquad (47)$$

The equations form a set of linear equations in the unknown secondary moments Q_j; the cable profile appears only on the right-hand side of the equations, and the coefficients of the Q_j terms are integrals of products of the β functions, many of which are zero. Of the non-zero terms, although they are formally integrals over the whole length of the beam, only the spans (at most two) over which both β_i and β_j are non-zero need to be considered.

82. Equations (47) are perfectly general, allowing the prestress force, eccentricity and stiffness to vary, but if EI is constant, the integrals on the left-hand side can be performed analytically. Simple algebra then yields

$$\frac{1}{6}\begin{bmatrix} 2(L_1 + L_2) & L_2 & \cdots & \cdots & \cdots \\ L_2 & 2(L_2 + L_3) & L_3 & \cdots & \cdots \\ \cdots & L_3 & 2(L_3 + L_4) & L_4 & \cdots \\ \cdots & \cdots & L_4 & \text{etc.} & \end{bmatrix} Q_j = \int \beta_i Pe \, dx = J_i \qquad (48)$$

The right-hand side terms (J_i) can be found by numerical integration. Because the β_i terms are zero, other than in the spans adjacent to the support in question, the integrals for each J_i need only consider two spans.

References

1. LEONHARDT F. *Prestressed concrete, design and construction.* Ernst & Sohn, Munich, 1948.
2. LIN T. Y. and BURNS N. H. *Design of prestressed concrete structures.* Wiley, New York, 1981.
3. NAAMAN A. E. *Prestressed concrete analysis and design fundamentals.* McGraw Hill, New York, 1982.
4. LOW A. McC. The preliminary design of prestressed concrete viaducts. *Proc. Instn Civ. Engrs*, Part 2, 1982, **73**, June, 351–364.
5. LOW A. McC. Prestress deisgn for continuous concrete members. *Arup Journal*, 1983, **18**, No. 1, Apr., 18–21.
6. MAGNEL G. *Prestressed concrete.* Concrete publications, London, 1948.
7. KONG F. K. and EVANS R. H. *Reinforced and prestressed concrete.* Nelson, 1975, 220.
8. DEPARTMENT OF TRANSPORT. *Loads for highway bridges, use of BS 5400: Part 2: 1978.* As modified by draft Departmental standard, Department of Transport, Roads and local transport directorate, 1984.
9. BURGOYNE C. J. Calculation of moment and shear envelopes by Macauley's method. *Engng Computations*, 1987, **4**, No. 3, Sept., 247–256.
10. BURGOYNE C. J. Automated determination of concordant profiles. To be published *Proc. Instn Civ. Engrs*, Part 2.

Proc. Instn Civ. Engrs, Part 2, 1988, **85**, Dec., 737–738

Cable design for continuous prestressed concrete bridges

C. J. Burgoyne

Mr A. McC. Low, *Ove Arup and Partners, London*

This extension to the published theory on this topic is to be welcomed, and I have one comment. Fig. 10 shows the limits on prestressing force along the 3-span bridge example. The maximum force shown is calculated from the extremity of the Magnel diagram. This could be called $P_{1\text{max}}$. What is missing is the maximum force limits imposed by case 3, $P_{3\text{max}}$. Following arguments similar to those in § 8 of the Paper and in §§ 15–20 of reference 4, it can be shown that for an internal span

$$P_{3\text{max}} = f_{\text{cw}} A - \frac{\bar{M}_{\text{LH}} A}{Z_{\text{B}}} = \frac{Z_2 f_{\text{cw}} - \bar{M}_{\text{a}}}{Z_2/A} \qquad (49)$$

84. From Fig. 7, it may be judged that for the centre span $\bar{M}_{\text{LH}} \simeq 0{\cdot}5 \times \bar{M}_{\text{LS}}$. Hence $P_{3\text{max}} \simeq 6{\cdot}616 \times 16{\cdot}5 - 0{\cdot}5 \times 51{\cdot}82 = 83{\cdot}3$ MN. This is much less than the values of P_{max} plotted in Fig. 10. A similar derivation is possible for the end spans.

85. Introducing the concept of maximum cable force in continuous spans raises some interesting questions. Are cases 1 and 3 the only cases to impose maximum limits? Cases 2 and 4 are both governed by the limit on the cable profile amplitude. When there is an excess of force this will not govern. Hence cases 2 and 4 govern P_{min} but not P_{max}. Are there complementary cases 5 and 6 which govern P_{max} but not P_{min}?

Dr Burgoyne

It is quite correct to state that other criteria could be derived. In the Paper, equation (19) was derived on the assumption that e_{min} is the limiting position of the line of thrust, and that this condition is governed by tensile stresses in the bottom fibre under the action of the maximum applied moment M_{b}. *Mr Low*'s condition (49) is derived on the assumption that e_{max} is the limiting position, and that this is governed by compressive stresses in the bottom fibre under the action of the minimum applied moment M_{a}.

87. Clearly, there are many other similar relationships that could be derived, but this should not be allowed to detract from the main point of the argument: the prestressing force must be chosen such that a cable placed at e_{min} would give rise to hogging secondary moments, while one placed at e_{max} would give rise to sagging secondary moments. Under those circumstances, a concordant line of thrust between e_{max} and e_{min} can exist.

Paper published: *Proc. Instn Civ. Engrs*, Part 2, 1988, **85**, Mar., 161–184.

88. Mr Low raises the possibility that upper limits might exist on the cable force that correspond to the lower limits imposed by P_2 and P_4. This is not the case, however, since P_2 and P_4 are limited by the maximum eccentricity determined by the section dimensions. Increasing the cable force decreases the eccentricity, and there are no corresponding lower limits on eccentricity that need to be introduced. There is no need to worry about possible limits on P_5 and P_6.